



OPEN

A mutation in the intron splice acceptor site of a *GA3ox* gene confers dwarf architecture in watermelon (*Citrullus lanatus* L.)

Yuyan Sun, Huiqing Zhang, Min Fan[✉], Yanjun He & Pingan Guo

Dwarf architecture is an important trait associated with plant yield, lodging resistance and labor cost. Here, we aimed to identify a gene causing dwarfism in watermelon. The 'w106' (dwarf) and 'Charleston Gray' (vine) were used as parents to construct F_1 and F_2 progeny. Dwarf architecture of 'w106' was mainly caused by longitudinal cell length reduction and was controlled by a single recessive gene. Whole-genome sequencing of two parents and two bulk DNAs of F_2 population localized this gene to a 2.63-Mb region on chromosome 9; this was further narrowed to a 541-kb region. Within this region, Cla015407, encoding a gibberellin 3 β -hydroxylase (*GA3ox*), was the candidate gene. Cla015407 had a SNP mutation (G \rightarrow A) in the splice acceptor site of the intron, leading to altered splicing event and generating two splicing isoforms in dwarf plants. One splicing isoform retained the intron sequences, while the other had a 13-bp deletion in the second exon of *GA3ox* transcript, both resulting in truncated proteins and loss of the functional Fe2OG dioxygenase domain in dwarf plants. RNA-Seq analysis indicated that expression of Cla015407 and other GA biosynthetic and metabolic genes were mostly up-regulated in the shoots of dwarf plants compared with vine plants in F_2 population. Measurement of endogenous GA levels indicated that bioactive GA_4 was significantly decreased in the shoots of dwarf plants. Moreover, the dwarf phenotype can be rescued by exogenous applications of GA_3 or GA_{4+7} , with the latter having a more distinct effect than the former. Subcellular localization analyses of *GA3ox* proteins from two parents revealed their subcellular targeting in nucleus and cytosol. Here, a *GA3ox* gene controlling dwarf architecture was identified, and loss function of *GA3ox* leads to GA_4 reduction and dwarfism phenotype in watermelon.

Plant height is an important agronomic trait that affects the quality and yield of plants¹. The cultivation of dwarf crops has been widely applied in wheat¹, rice², maize³, pea⁴ and peach⁵. At present, most vine watermelon (*Citrullus lanatus* L.) varieties are planted for commercial production. With the rapid spread of watermelon protection areas, it is a good opportunity for the selection and cultivation of dwarf watermelon. Dwarf watermelon have short shoots, and are easily cultivated and managed, allowing for an increase in planting density, which can lead to increased yields and financial benefits.

There are various mechanisms leading to plant dwarfism. Changes in biosynthesis or perception of plant hormones, such as gibberellin (GA)⁶, brassinosteroid⁷, auxin⁸ and strigolactone⁹ can cause plant dwarfism. Additionally, abnormal expression of transcription factors, such as HD-Zip II¹⁰, *WOX1*¹¹, *AP2*¹² and *GRAS*¹³ can also lead to dwarf architecture in plants.

GA is a kind of diterpenoid carboxylic acids that widely exist in plants, including the functional active molecules GA_1 , GA_3 , GA_4 and GA_7 , as well as the non-active molecules GA_9 , GA_{19} , GA_{20} , GA_{29} and GA_{51} ^{14,15}. GAs have a variety of biological functions, including promoting the stem elongation^{14,15}. In plants, GA biosynthesis and metabolism are catalyzed by six key enzymes, ent-copalyl diphosphate synthase (CPS), ent-kaurene synthase (KS), ent-kaurene oxidase (KO), ent-kaurenoic acid oxidase (KAO), GA 20-oxidase (*GA20ox*) and GA 3-oxidase (*GA3ox*), and its deactivation is catalyzed by GA 2-oxidase (*GA2ox*)^{14,15}. GAs could promote the stem elongation by stimulating the degradation of DELLA proteins¹⁶. Mutations in GA biosynthetic genes lead

Institute of Vegetables, Zhejiang Academy of Agricultural Sciences, Hangzhou 310021, China. ✉email: fanminfm@sina.com

to dwarfism by reducing the endogenous GA levels, leading to DELLA protein accumulation, and ultimately limiting internode elongation in plants⁵.

Among the six enzymes, GA20ox and GA3ox catalyze the final two steps of GA biosynthetic pathway, and GA2ox catalyzes the GA metabolic pathway^{17–19}. GA20ox, the “Green revolution gene” in rice, encodes a key enzyme that catalyzes the penultimate step of GA biosynthesis, converting GA₁₂ to GA₉, and GA₅₃ to GA₂₀¹⁷. Mutations in GA20ox genes conferring dwarf phenotypes have been reported in rice^{20,21}, barley^{22,23} and *Arabidopsis*^{24,25}. GA3ox catalyzes the final step of the GA biosynthetic pathway, converting GA₂₀ to GA₁, GA₉ to GA₄, and GA₅ to GA₃, which leads to the active molecules GAs¹⁸. Mutations of GA3ox genes have been identified in maize¹⁸, rice²⁶, *Arabidopsis*²⁷ and *Medicago sativa*²⁸, and they are causing the dwarf phenotypes in these plants. GA2ox catalyzes the deactivation of bioactive GAs or its precursors to inactive forms through 2β-hydroxylation reaction; thus, plays a direct role in the determination of bioactive GAs content¹⁹. The GA2ox genes leading to dwarf phenotypes have been reported in wheat⁶, switchgrass²⁹, rice³⁰ and tomato³¹.

Watermelon belongs to the *Cucurbitaceae* and is a diploid species with a chromosomal number of $2n = 2 \times 11$ and a genome size of 425 Mb³². Approximately 97 million tons of watermelon are produced worldwide each year, with China being the largest producer. Watermelon dwarf mutants have been identified and analyzed in previous studies. Dwarf mutants in watermelon are controlled by *dw-1*³³, *dw-1s*³⁴, *dw-2*³⁵, *dw-3*³⁶, *dsh*³⁷, *Cldf*³⁸, *dw*³⁹ and *Cldw-1*⁴⁰, and the dwarf traits were controlled by respective single recessive genes^{37–40}. At present, the *dsh* gene has been identified through whole-genome sequencing of two bulk DNAs, and Cla010726 (GA20ox) was predicted to be the candidate gene³⁷. In addition, a SNP mutation of GA3ox^{38,39} and a SNP deletion in an ABC transporter gene⁴⁰ also lead to dwarfism phenotypes in watermelon.

In recent years, the combination of a bulked segregant analysis (BSA) and next-generation sequencing technology (BSA-Seq) has been widely applied to identify candidate genes controlling important agronomic traits in watermelon, such as dwarf phenotype^{37–40}, lobed leaves⁴¹, yellow skin⁴², fruit shape⁴³, fruit pigment accumulation⁴⁴ and anthracnose resistance⁴⁵. In this study, we investigated the inheritance of watermelon dwarf genes in the F₂ population of ‘w106’ (dwarf) × ‘Charleston Gray’ (CG; vine), which indicated that the dwarf phenotype was controlled by a single recessive gene. The candidate gene, Cla015407 (GA3ox), was obtained through BSA-Seq and mapping analysis. A single nucleotide polymorphism (SNP) mutation (G → A) occurred in the splice acceptor site of the intron in Cla015407, which lead to altered splicing, resulting in two splicing isoforms in dwarf plants. This point mutation leads to loss function of GA3ox and GA₁ level reduction in dwarf plants. This study identify a GA3ox gene controlling dwarf architecture in watermelon and will aid in revealing the molecular mechanism of plant height in future.

Materials and methods

Plant materials. Two watermelon parental lines, ‘w106’ (dwarf) and ‘CG’ (vine), were used as the female and male parents, respectively. The F₁ plants were generated by crossing ‘w106’ and ‘CG’, and self-pollinated to produce the F₂ progeny. The 15 plants of each parental line, 15 F₁ plants and 98 F₂ plants were used for genetic analysis and BSA-Seq. For fine mapping, the dwarf individuals of a larger F₂ population were used. The cross and self-pollination were carried out at the Haining Base of Zhejiang Academy of Agricultural Sciences. The plants used for the genetic analysis, BSA-Seq and fine mapping were grown and evaluated in a greenhouse at Zhejiang Academy of Agricultural Sciences.

Analysis of shoot sections. Shoots of dwarf and vine plants were fixed with 50% FAA for 24 h at 4 °C. Subsequently, these samples were dehydrated in a graded ethanol series, infiltrated with xylene and embedded in paraffin. Sections were sliced using an ultramicrotome and stained with safranin and fast green, and finally, observed under an optical microscope.

Bulk DNA construction and Illumina sequencing. DNAs were extracted using the CTAB method from leaves of both parental lines and F₂ plants for BSA-Seq. Two bulk DNA samples, dwarf bulk (D-bulk) and vine bulk (V-bulk), were constructed by mixing equal amounts of DNAs from 25 dwarf plants and 25 vine plants from the F₂ population, respectively. Paired-end DNA libraries were prepared according to the manufacturer’s instructions (Truseq Library Construction; Illumina, San Diego, CA, USA). First, genomic DNA was sheared into 350-bp fragments using a Covaris S220 sonicator (Woburn, MA, USA). Second, ends of the gDNA fragments were repaired, and 3’ ends were adenylated. Then, the size distributions and concentrations of the libraries were determined using an Agilent 2100 Bioanalyzer (Agilent Technologies, Waldbronn, Germany) and quantified by real-time PCR. Finally, DNA libraries were sequenced using an Illumina HiSeq X at Genepioneer (Nanjing, Jiangsu, China) according to the manufacturer’s instructions for paired-end 150-bp reads.

The short reads from D-bulk and V-bulk were aligned to the ‘97103’ reference genome³² using BWA software⁴⁶. Alignment files were converted to SAM/BAM files using SAM tools⁴⁷. SNPs and Insertion/deletion polymorphisms (InDels) were also assessed.

Gene location association analysis. All samples underwent variant calling using the Unified Genotyper function of the GATK program⁴⁸. The SNPs and InDels were filtered using the Variant Filtration parameter of GATK. ANNOVAR, which is an efficient software tool, was used to annotate the SNPs or InDels based on the GFF3 files for the reference genome⁴⁹. The homozygous SNPs/InDels between two parental lines were extracted from the vcf files.

A SNP index was used to indicate the proportion of reads harboring SNPs that differed from reference sequences⁵⁰. An Euclidean distance (ED) value was calculated by comparing SNPs across the two bulk DNAs as follows: $\text{SNP-index}_{\text{alt}} = N_{\text{alt}} / (N_{\text{alt}} + N_{\text{ref}})$, $\Delta(\text{SNP-index}_{\text{alt}}) = \text{SNP-index}_{\text{alt}}(\text{V-bulk}) - \text{SNP-index}_{\text{alt}}(\text{D-bulk})$,

$\text{SNP-index}_{\text{ref}} = N_{\text{ref}} / (N_{\text{alt}} + N_{\text{ref}})$, $\Delta(\text{SNP-index}_{\text{ref}}) = \text{SNP-index}_{\text{ref}}(\text{V-bulk}) - \text{SNP-index}_{\text{ref}}(\text{D-bulk})$ and $\text{ED} = [\Delta(\text{SNP-index}_{\text{ref}})^2 + \Delta(\text{SNP-index}_{\text{alt}})^2]^{1/251}$. Using these formulae, we assessed whether the measured values fell within the following ranges, $-1 \leq \Delta(\text{SNP-index}) \leq 1$ and $0 \leq \text{ED} \leq 1.414^{51,52}$. The greater of the ED value, the closer of the object site⁵². The $\Delta(\text{InDel-index})$ and EDs of InDel sites were calculated using the InDel-index⁵³ as described above for calculating for SNP regions. Using a 1-kb sliding window, an average SNP/InDel-index was calculated over a 1-Mb interval.

Mapping of the candidate gene. To minimize the genetic interval and verify the accuracy of BSA-Seq, 161 simple sequence repeat (SSR) markers within the BSA-Seq region were developed based on the whole-genome sequencing of the two parental lines. These newly developed SSR markers were first screened for polymorphisms between the two bulk DNAs, then the polymorphic SSRs were used to screen for recombinants in the dwarf individuals of the F₂ population.

The PCR was carried out in a total volume of 15 μL containing 7.5 μL 2 \times TSINGKE Master Mix (Tsingke, Beijing, China), 0.5 μL of each primer (10 μM), 2 μL genomic DNA (~ 50 ng/ μL) and 4.5 μL sterilized ddH₂O. All the amplifications were performed on a Mastercycler nexus GSX1 (Eppendorf, Germany) under the following conditions: 95 $^{\circ}\text{C}$ for 5 min; 33 cycles of 30 s at 95 $^{\circ}\text{C}$, 45 s at 55 $^{\circ}\text{C}$ and 45 s at 72 $^{\circ}\text{C}$, followed by a final extension step at 72 $^{\circ}\text{C}$ for 10 min. The amplified products were separated on 8.0% non-denatured polyacrylamide gel with electrophoresis at 150 V constant power for 1 h. After fixation in 10% ethanol + 0.5% glacial acetic acid for 10 min, the silver staining in 0.2% AgNO₃ for 12 min was performed. Samples were then rinsed in distilled water for 1 min and 1.5% NaOH + 0.4% formaldehyde for 6 min. The band pattern analysis was performed under a GL-800 Compact White Light Transmissometer (Kylin-Bell, Haimen, Jiangsu, China).

Cloning and sequence analysis of candidate gene. Total DNAs and RNAs were extracted from leaves of two parental plants using CTAB and TRIzol Reagent (Invitrogen, Carlsbad, CA, USA), respectively. First-strand cDNA was synthesized using a FastKing RT Kit (with gDNase) (Tiangen Biotech, Beijing, China). The PCR was carried out in a total volume of 25 μL containing 12.5 μL 2 \times PCR buffer for KOD FX (Toyobo, Osaka, Japan), 0.5 μL KOD FX (1.0 U/ μL) (Toyobo), 5.0 μL dNTPs (2 mM) (Toyobo), 0.5 μL of each primer (10 μM) (F: 5'-ATGGGAAGCATCAAATAACCG-3'; R: 5'-TTAACCTACTTTAACCTGGCTG-3'), 2.0 μL cDNA (50 ng/ μL) and 4.0 μL sterilized ddH₂O. Amplifications of candidate genes were performed under the following conditions: 95 $^{\circ}\text{C}$ for 5 min; 33 cycles of 30 s at 95 $^{\circ}\text{C}$, 45 s at 55 $^{\circ}\text{C}$ and 45 s at 72 $^{\circ}\text{C}$, followed by a final extension step at 72 $^{\circ}\text{C}$ for 10 min. Amplification products were analyzed on 1.5% agarose gel and sent for sequencing.

Transcriptome sequencing of dwarf and vine plants. Transcriptome sequencing (RNA-Seq) was performed to analyze the expression of candidate genes and reveal the related pathways involved in dwarf architecture. Total RNAs were extracted from shoots of dwarf and vine plants in the F₂ population using TRIzol Reagent (Invitrogen, Carlsbad, CA, USA). Approximately 10 μg total RNA was subjected to Poly(A) mRNA isolation using poly-T oligo-attached magnetic beads (Invitrogen, Carlsbad, CA, USA). Following purification, the mRNA was fragmented into small pieces and the cleaved RNA fragments were reverse-transcribed to create the final cDNA library. The average insert size for the paired-end libraries was 300 bp (± 50 bp). Then, the paired-end sequencing was performed on an Illumina HiSeq 4000 platform at Genepioneer (Nanjing, Jiangsu, China) following the vendor's recommended protocol. Triplicates of each sample were carried out for Illumina sequencing.

Gene expression was assessed using the fragments per kilobase of transcript per million fragments mapped (FPKM) method⁵⁴. The differentially expressed genes (DEGs) were determined using the criterion $|\log_2(\text{Fold Change})| \geq 1$ and $\text{FDR} < 0.05$. The corresponding functions were revealed using the KEGG Automatic Annotation Server⁵⁵.

Measurement of endogenous GA levels using internal standards. At the fourth-true leaf stage, the shoots of vine and dwarf plants in two parents and F₂ population grown under the same condition were harvested. The endogenous levels of 18 kinds of GAs involved in GA biosynthetic and metabolic pathway (GA₁, GA₃, GA₄, GA₅, GA₆, GA₇, GA₈, GA₉, GA₁₂, GA₁₅, GA₁₉, GA₂₀, GA₂₄, GA₂₉, GA₃₄, GA₄₄, GA₅₁ and GA₅₃) were measured using 2H₂-GA internal standards coupled with UPLC-MS/MS analyses at LC Sciences (Hangzhou, China). For the measurement, shoots from three seedlings of vine and dwarf plants were mixed and ground into fine powder in liquid nitrogen, respectively; weighed ~ 100 mg sample, added 1.0 ng/g corresponding 2H₂-GA internal standards and 1 mL methanol/water (80/20, v/v) extracting solution at 4 $^{\circ}\text{C}$ for overnight, then centrifuged at 10,000 $\times g$ for 20 min at 4 $^{\circ}\text{C}$; the supernatant was taken and absorbed through the C18/SAX solid-phase extraction column; 2 mL methanol/water (20/80, v/v) was used to clean the SAX extraction column, and 3 mL ACN/FA (99/1, v/v) was used to desorb the target acid plant hormones retained on the SAX extraction column; the desorption solution was blow-dried with constant nitrogen flow at 40 $^{\circ}\text{C}$ and redissolved in 100 μL water, and 10 μL FA was added to the 100 μL solution and extracted twice with ether; the extracted organic phase was combined and blow-dried by nitrogen at room temperature, then dissolved in 100 μL ACN; adding 10 μL \times 20 $\mu\text{mol}/\text{mL}$ TEA and 10 μL \times 20 $\mu\text{mol}/\text{mL}$ BTA to the ACN solution, swirl for 35 min at room temperature and then blow-dried with nitrogen; redissolved the solution in 200 μL H₂O/ACN (90/10, v/v) for subsequent UPLC-MS/MS analyses. The UPLC-MS/MS analyses were performed on Thermo Scientific Ultimate 3000-Thermo Scientific TSQ Quantiva. Three biological replicates were conducted for each measurement, and endogenous levels of GAs (ng/g fresh weight) were determined by means of three UPLC-MS/MS detection results. T-test was conducted for statistical analysis using SAS 8.0. The GAs with $|\log_2(\text{Fold(FC)})| \geq 1$ and statistical significance (p value < 0.05) were considered as significant difference.

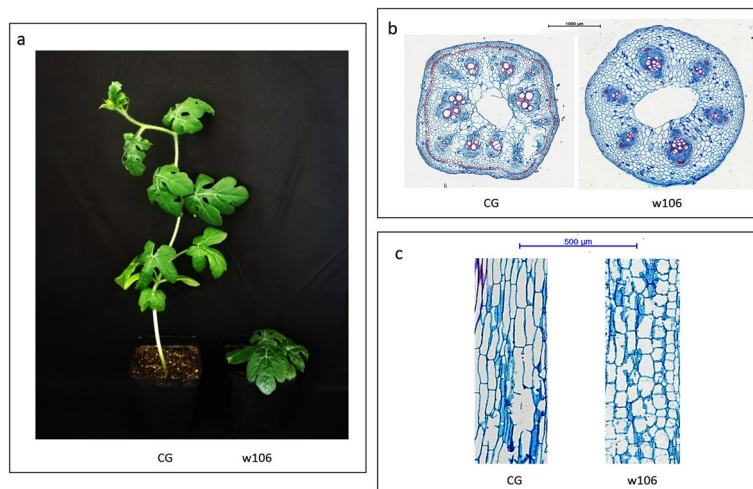


Figure 1. Phenotypic characterization and morphological analysis of two parental lines used in present study. (a) Phenotypic characterization of the two parental lines. Shoot length are reduced in ‘w106’ (right) as compared to ‘CG’ (left). (b) Transverse sections of shoots in two parental lines. (c) Longitudinal sections of shoots in two parental lines. The ‘w106’ (right) showed reduced longitudinal cell length compared with ‘CG’ (left).

Exogenous treatments with GA₃ or GA₄₊₇. In addition, the dwarf parental lines were employed to assess responses to exogenous application of GAs. The GA₃ (Ryon, Shanghai, China) and GA₄₊₇ (Ryon, Shanghai, China) are independently dissolved in a small amount of ethanol and then diluted with sterilized ddH₂O to the final concentration of 500 μM. The seedlings were sprayed independently with 500 μM GA₃ or GA₄₊₇ for four times at 3-day intervals. The control seedlings were sprayed with sterilized ddH₂O. Three seedling were used for each treatment. The phenotypes of seedlings were analyzed and photographed 3-days after the last GA treatment.

Subcellular localization analyses of GA3ox protein. The CDS sequences of Cla015407 from ‘CG’ and ‘w106’ were amplified using gene-specific primer (F: 5'-CGGGATCCCCGATGGGAAGCATCAAATAAC-3'; R: 5'-GCTCTAGAGCTTAACCTACTTTAACCTGGCTG-3') and cloned into the pFGC-eGFP plasmid via the BamH I and Xba I restriction sites. These recombinant plasmids were transformed into *Agrobacterium tumefaciens* GV3101 and transiently expressed in tobacco leaf cells. Images were acquired at 48 h using a Leica DMLE camera (Leica, Wetzlar, Germany).

Ethical standards. The authors declare that this study complies with the current laws of the countries in which the experiments were performed.

Results

Phenotypic and genetic analyses. The height of ‘w106’ was significant shorter than that of ‘CG’ (Fig. 1a). Therefore, we conducted a microscopic observation of shoots of the ‘CG’ and ‘w106’ plants using paraffin sectioning. The cell sizes in transverse sections were not obviously different between the ‘CG’ and ‘w106’ plants (Fig. 1b). However, the cell lengths in longitudinal sections were obviously shorter in ‘w106’ than in ‘CG’ plants (Fig. 1c). Thus, the defective cell elongation appears to be the main cause for the reduced shoots and dwarf architecture in watermelon.

To assess the inheritance of the dwarf trait in watermelon, crosses were made between ‘w106’ and ‘CG’. All the F₁ plants showed the vine phenotype. Among the 98 F₂ progeny, 72 individuals showed vine phenotype and 26 individuals showed dwarf phenotype, with the Chi-square test (χ^2) confirming the segregation ratio to be 3:1 (Table 1). These results indicated that the dwarf trait in ‘w106’ was controlled by a single recessive gene, designated as the *short internode* (*Si*) locus.

***Si* gene located on chromosome 9 (0.80–3.43 Mb) using BSA-seq.** We sequenced the genomes of the two parental lines and two bulk DNAs using the Illumina HiSeq™ PE150 platform. The high-throughput sequencing results obtained 50.30, 61.89, 65.48 and 70.68 Mb clean reads for female parent, male parent, D-bulk and V-bulk, respectively (Table 2). A total of 33.65 Gb clean data were generated for the two parental lines, and 40.84 Gb clean data were generated for the two DNA bulks, with approximately 42–57× sequencing depth and more than 99.00% 5× coverage per sample (Table 2). Data were aligned to the reference genome of watermelon ‘97103’ (<https://cucurbitgenomics.org/organism/1>), and 160,957 SNPs and 55,055 InDels, at a minimum of 5 reads, were identified between D-bulk and V-bulk. Each identified SNP or InDel was used to compute an SNP/InDel-index. The graph for $\Delta(\text{SNP}/\text{InDel-index})$ was plotted and computed against the genome positions by combining SNP/InDel-index of D-bulk and V-bulk (Fig. 2a,b). At the 99% significance level, the $\Delta(\text{SNP-index})$

Plants	Number of total plants	Number of vine plants	Number of dwarf plants	$\chi^2_{3:1}$	$\chi^2_{0.05}$
'w106' (female; dwarf)	15	0	15		
'CG' (male; vine)	15	15	0		
F ₁	15	15	0		
F ₂	98	72	26	0.683	3.841

Table 1. Genetic analysis of the dwarf trait in watermelon. $\chi^2_{3:1} < \chi^2_{0.05} = 3.841$, indicating that dwarf trait in 'w106' was controlled by a single recessive gene.

Samples	Number of reads (M)	Clean reads (M)	Clean data (G)	Q20 (%)	Q30 (%)	Average depth	Coverage ($\geq 5\times$) (%)
'w106' (female)	102.32	50.30	15.09	96.64	91.00	42.87	99.44
'CG' (male)	126.70	61.89	18.56	96.78	91.31	50.93	99.45
D-bulk	133.59	65.48	19.64	96.78	91.31	55.09	99.48
V-bulk	144.67	70.68	21.20	96.99	91.79	57.95	99.48

Table 2. Summary of sequencing data for two parental lines and two DNA bulks in F₂ population.

and $\Delta(\text{InDel-index})$ values located the region on chromosome 9 (0.72–3.93 Mb) and chromosome 9 (0.80–3.43 Mb), respectively (Fig. 2a,b; Supplementary Table S2). The results indicated that a candidate gene controlling the dwarf trait in 'w106' was located in the 0.80–3.43 Mb region of chromosome 9 (Fig. 2c).

Further mapping analysis narrowed *Si* to a 541-kb interval and a candidate gene was predicted.

To further narrow down the location of the *Si* locus detected by BSA-Seq, we selected 161 SSR markers from chromosome 9 (0.80–3.43 Mb) based on resequencing data of the two parental lines. All these SSR markers were first screened for polymorphisms between the two bulk DNA samples, and then, 16 polymorphic markers were applied to screen recombinants of the dwarf individuals in the F₂ population. Finally, two flanking markers, dw37 (Chr9:1620039) and dw134 (Chr9:2161629), obtaining one and four recombinants, respectively, placed the *Si* locus in a 541-kb region (Fig. 2d). Additionally, no recombinant was obtained using the marker dw128 (Chr9:1835342), indicating that the target gene neighbored dw128. All the polymorphic SSR markers used in this study and the obtained recombinants are listed in Supplementary Table S3.

According to the watermelon genome annotation, 66 putative genes (Cla015361–Cla015427) were detected within the 541-kb interval (Supplementary Table S4). Within this region, three SNPs and one InDel were identified among the two parental lines and two bulk DNAs according to the whole-genome sequencing data (Table 3). Among these four variations, two SNP variations (Chr9:1620753 and Chr9:1621230) occurred in the intergenic region of the genome and an InDel (Chr9:1996536) occurred in the upstream of Cla015387 (WD43). One SNP occurred in Chr9:1857472 (from 'G' in 'CG' to 'A' in 'w106'), locating at the splice-site acceptor in the intron of Cla015407 (Fig. 2e; Table 3). Cla015407 encodes GA3ox, which is involved in the GA biosynthetic pathway. Additionally, the genome location of Cla015407 (Chr9:1856847–1858103) neighbored the SSR marker dw128 (Chr9:1835342), which did not identify any recombinants and was near the target gene. Therefore, Cla015407 was predicted to be the candidate gene conferring the dwarf architecture of 'w106'.

Sequences analyses of the candidate gene. To verify the sequences of Cla015407 at the DNA and mRNA levels, we cloned the DNA and coding sequence (CDS) of Cla015407 from both parental lines. Fragments of 1,257 bp were amplified at the DNA level from both parental lines (Fig. 3a), and the sequencing analysis further verified the G → A variation at the 626th nucleotide of Cla015407 (Fig. 3c).

At the cDNA level, a fragment was amplified from vine parent 'CG' and two fragments were amplified from dwarf parent 'w106', which indicated that this SNP mutation lead to altered splicing, generating two splicing isoforms in the dwarf plants (Fig. 3b). Sequence analyses of the splicing isoforms in 'w106' revealed that the full-length isoform (isoform 1) retained the intron sequences and contained the premature termination codon 'TAG' at the 505–507th nucleotides (Fig. 3d). Additionally, the truncated isoform (isoform 2) had a 13-bp deletion in the second exon compared with the CDS of 'CG' and contained the premature termination codon 'TGA' at the 520–522th nucleotides (Fig. 3d).

The proteins encoded by the transcripts of Cla015407 in vine and dwarf parents were also predicted. The transcript of Cla015407 in vine parent 'CG' encodes a protein with 377 aa (Fig. 3e). However, the full-length isoform (isoform 1) in the dwarf parent 'w106' contains an unspliced intron, introducing a stop codon (TAG) just after the splice donor site, thus translation of this full-length transcript is prematurely terminated and produces a protein with 168 aa (Fig. 3e). Moreover, the truncated isoform (isoform 2) has a 13-bp deletion in the second exon of Cla015407 in dwarf parent 'w106' and contains a premature termination codon 'TAG' at 520–522th nucleotides, leading to frame shift and premature termination, and resulted in a truncated protein with 173

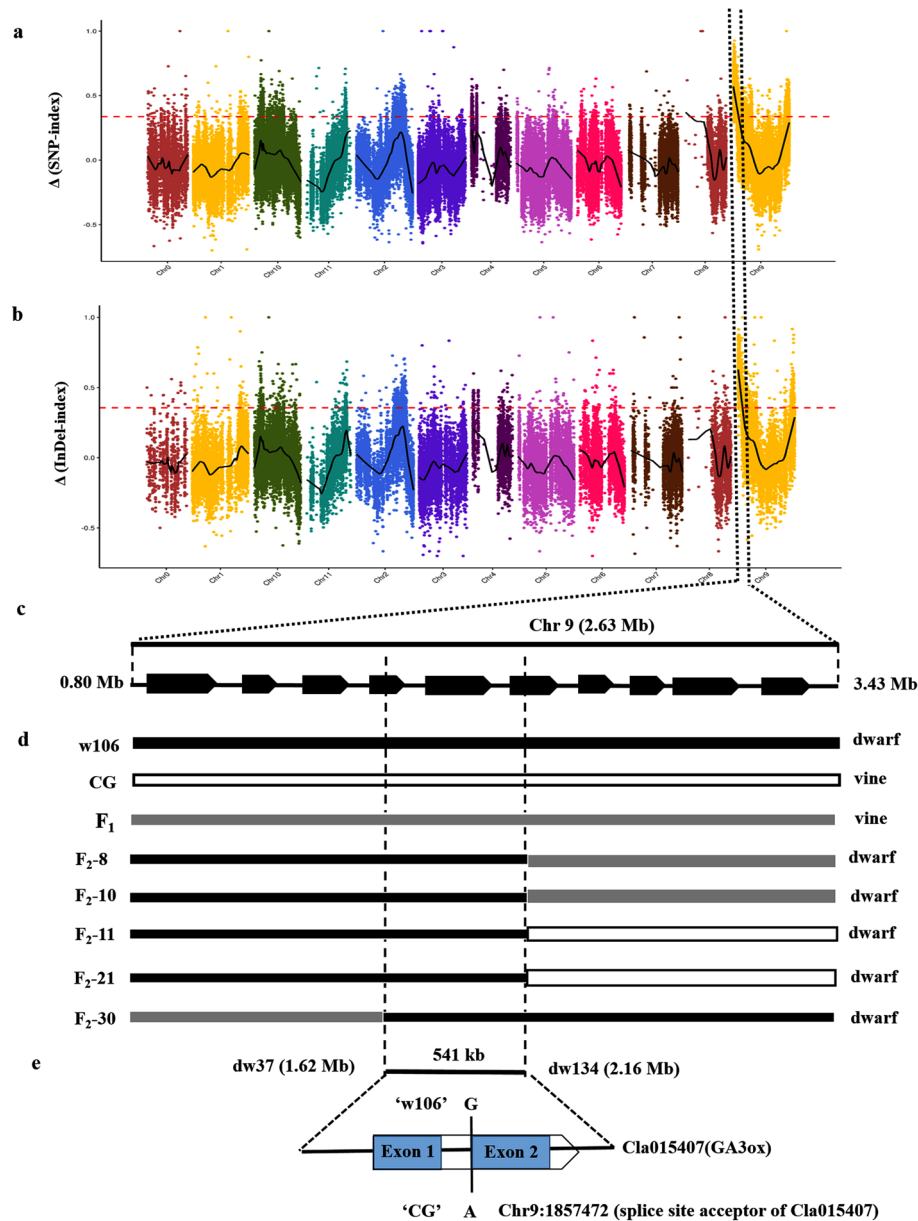


Figure 2. Genetic mapping and prediction of the *Si* locus in watermelon by BSA-Seq and mapping analysis. (a) $\Delta(\text{SNP-index})$ graph of BSA-Seq analysis. (b) $\Delta(\text{InDel-index})$ graph of BSA-Seq analysis. (c) Locus at the interval of 0.80–3.43 Mb on chromosome 9 was identified to control watermelon dwarf trait by combining the $\Delta(\text{SNP-index})$ and $\Delta(\text{InDel-index})$ of BSA-Seq analysis. The *x*-axis represents the position of watermelon chromosomes. The *y*-axis represents the value of Δ -index for SNPs and InDels. The scatter in the figure indicates that the value of Δ -index is calculated. The black curve represents the fitting value of Δ -index and the pink dotted line represents a threshold line with an snpnum smooth fitting value of 99%. (d) Screening of recombinants in F₂ progeny delimited the location of *Si* in an interval of 541-kb by two SSR markers dw37 and dw134. (e) Within the 541-kb interval, a SNP change occurring in the splice site acceptor for the intron of *Cla015407*, which encodes the GA3ox protein.

aa residues (Fig. 3e). In summary, the two transcripts of *Cl015407* from the dwarf plants resulted in truncated proteins and lost the functional Fe2OG dioxygenase domain.

DEGs identification between dwarf and vine plants and their KEGG pathway enrichment analyses. Transcriptome analyses of the shoots for dwarf and vine plants in the F₂ population were carried out to reveal the expression patterns of the candidate gene and GA biosynthetic and metabolic genes. A total of 3,027 genes showed differential expression, with 1,144 up-regulated and 1,883 down-regulated in dwarf plants com-

Variation types	Positions	'w106' (dwarf)	'CG' (vine)	D-bulk	V-bulk	Effect	Codon change / distance	Gene ID	Nr_annotation
SNP	Chr9:1620753	A, A	G, G	A, A	A, G	Intergenic	-	-	
SNP	Chr9:1621230	T, T	C, C	T, T	T, C	Intergenic	-	-	
SNP	Chr9:1857472	A, A	G, G	A, A	G, A	Splice site acceptor	Exon_2	Cla015407	Gibberellin 3β-hydroxylase
InDel	Chr9:1996536	AT, AT	ATAC, ATAC	AT, ATAC	ATAC, ATAC	Upstream	286	Cla015387	WD repeat-containing protein 43

Table 3. SNP and InDel variations within the region on Chr9 (1.62–2.16 Mb). *Intergenic* DNA sequences located between genes (no transcript), *splice site acceptor* splice donor mutation (within 2 bp before exon), *Upstream* upstream gene region (within 5-kb), *Codon change/distance* coding changes (old_codon/new_codon) or mutation distance to transcript (upstream and downstream region of gene).

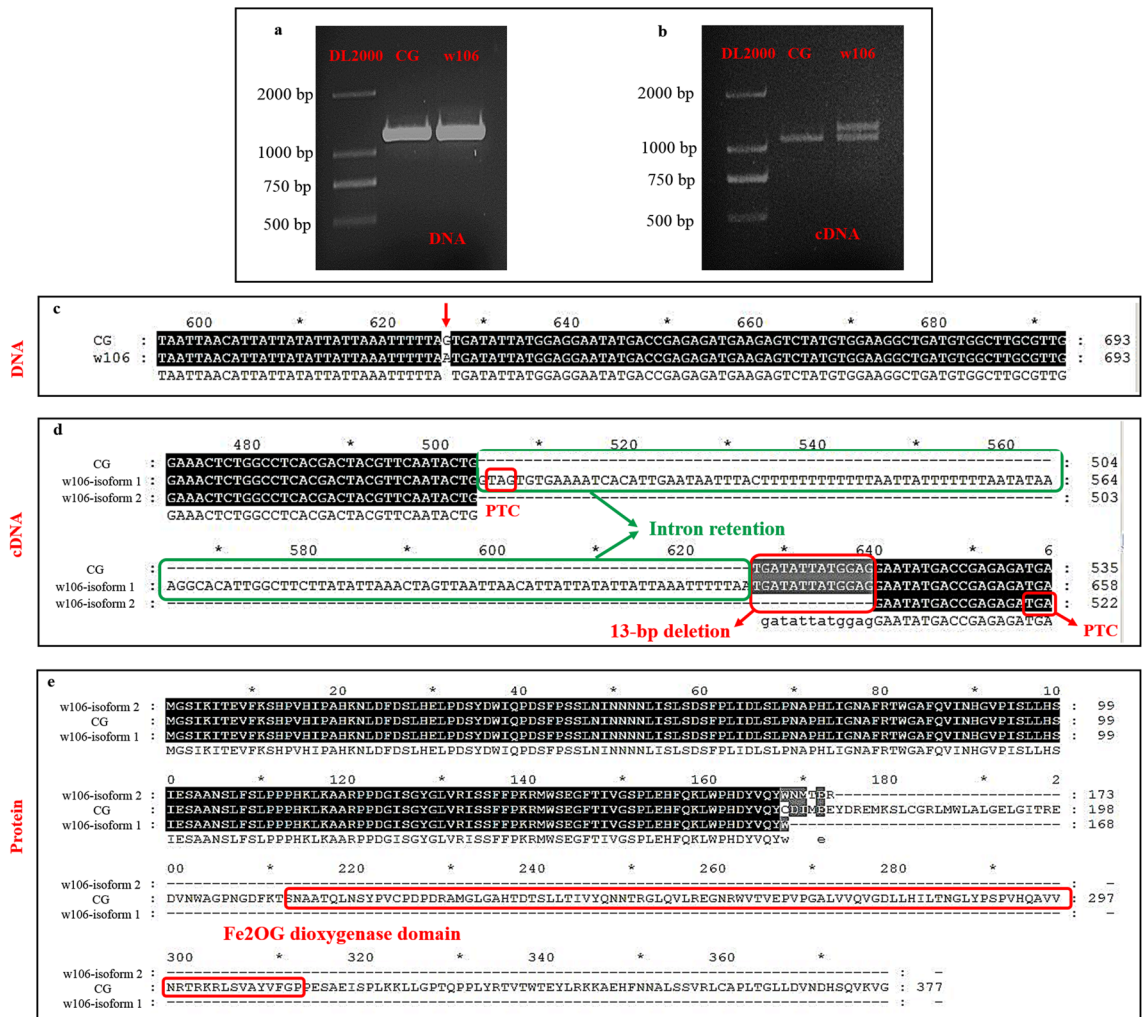


Figure 3. Sequence analysis of Cla015407 from two parental lines. (a) Amplifications of Cla015407 in two parental lines on DNA level. (b) Amplifications of Cla015407 in two parental lines on cDNA level. (c) Sequencing results verified the SNP (G → A) in 'CG' and 'w106' on DNA level at 626th nucleotide. (d) Sequencing results of two splicing isoforms on cDNA level in 'w106' indicated that the full-length isoform retained the intron sequence and the truncated isoform had 13-bp deletion at the second exon compared with the CDS in 'CG'. (e) Amino acids prediction of the two splicing isoforms indicated the loss of Fe2OG dioxygenase domain in 'w106' compared with 'CG'.

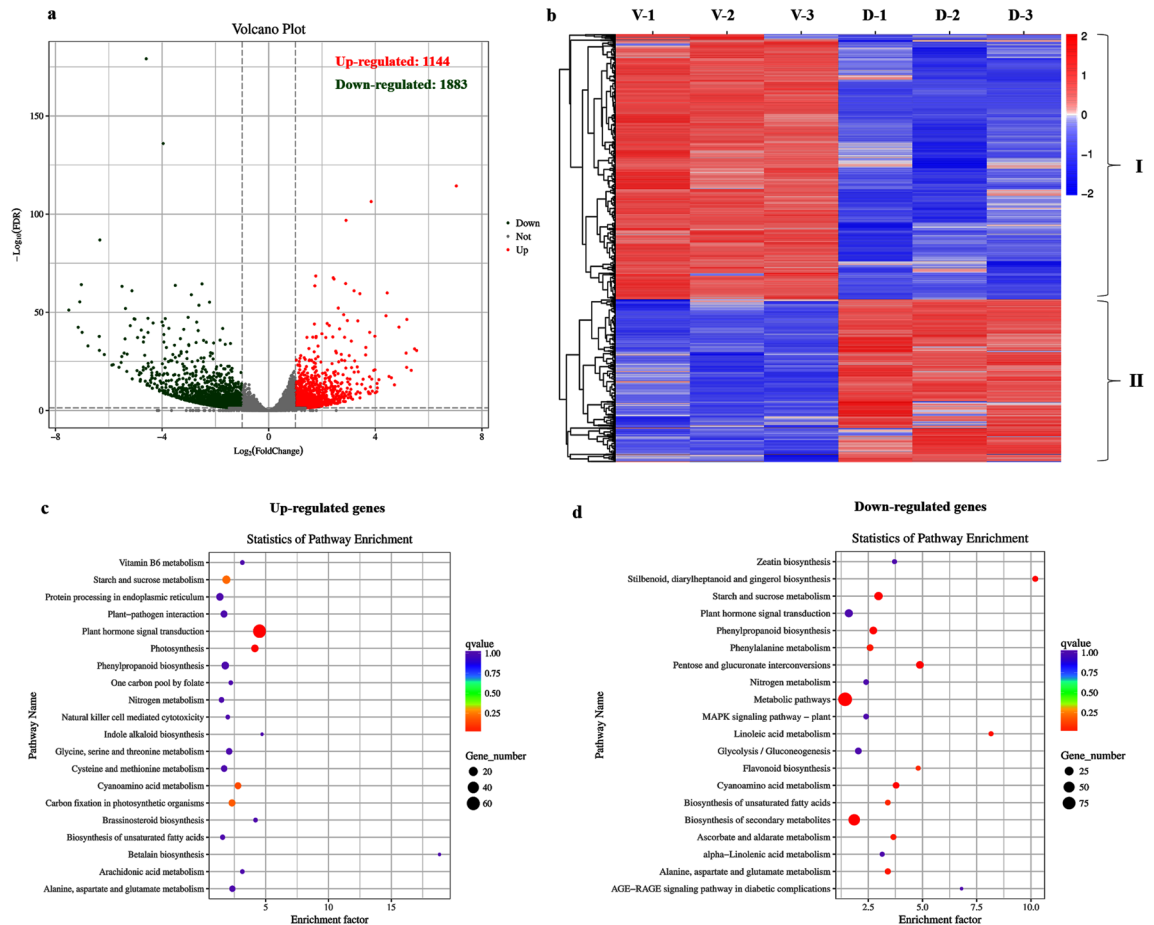


Figure 4. Volcano plot and heatmap of DEGs and their functional analysis. **(a)** Volcano plot of DEGs for vine plants and dwarf plants in F₂ population. **(b)** Heatmap of DEGs for vine plants and dwarf plants in F₂ population. The expression of DEGs were indicated by log₂(FPKM + 0.001). **(c)** The KEGG pathways enriched for the up-regulated genes in dwarf plants compared with vine plants. **(d)** The KEGG pathways enriched for the down-regulated genes in dwarf plants compared with vine plants. The size of each circle represents the number of significantly DEGs enriched in the corresponding pathway. The enrichment factor was calculated using the number of enriched genes divided by the total number of background genes in the corresponding pathway. The *q* value was calculated using the Benjamini–Hochberg correction. A pathway with *q* < 0.05 is considered significantly overrepresented.

pared with vine plants (Fig. 4a). In addition, the heatmap generating by Cluster 3.0 clearly divided these 3,017 DEGs into two Clusters (I and II) (Fig. 4b).

The KEGG pathway enrichment analyses were carried out for these DEGs (Fig. 4c,d). The up-regulated genes in dwarf plants were significantly enriched in KEGG pathways of ‘plant hormone signal transduction’ and ‘photosynthesis’ (Fig. 4c). Moreover, the down-regulated genes in dwarf plants were significantly enriched in KEGG pathways of ‘pentose and glucuronate interconversions’, ‘biosynthesis of secondary metabolites’, ‘stilbenoid, diarylheptanoid and gingerol biosynthesis’, ‘starch and sucrose metabolism’, ‘metabolic pathways’, ‘phenylpropanoid biosynthesis’, ‘cyanoamino acid metabolism’, ‘linoleic acid metabolism’, ‘alanine, aspartate and glutamate metabolism’, ‘ascorbate and aldarate metabolism’, and ‘phenylalanine metabolism’ (Fig. 4d).

Expression of GA biosynthetic and metabolic genes and phylogenetic analysis. As shown in Table 4, a total of 20 genes involved in GA biosynthesis and metabolism were detected as expressed at least one library, including one gene for CPS, one gene for KS, one gene for KO, two genes for KAO, six genes for GA20ox, two genes for GA3ox and seven genes for GA2ox. Most of these GA biosynthetic and metabolic genes in dwarf plants showed higher expression levels than those of vine plants. The expression of our candidate gene, Cla015407 (*GA3ox*), was significantly increased in dwarf plants. Moreover, one KO gene (Cla020710) and three *GA20ox* genes (Cla002362, Cla006227 and Cla008413) involved in GA biosynthesis, and two *GA2ox* gene (Cla015162 and Cla019586) involved in GA metabolism, were also significantly up-regulated in dwarf plants compared with those in vine plants.

Additionally, phylogenetic analysis of these *GA20ox*, *GA3ox* and *GA2ox* proteins in watermelon were carried out with a few selected *GA20ox*, *GA3ox* and *GA2ox* families in *Arabidopsis* and divided them into three major subgroups (I, II and III) (Supplementary Fig. S1). Subgroup I contained five watermelon *GA20ox*

Gene	Annotation	FPKM						Up/down-regulation
		V-1	V-2	V-3	D-1	D-2	D-3	
Cla006048	Ent-copalyl diphosphate synthase (CPS)	4.76	10.14	5.55	7.06	6.49	8.06	Up
Cla005482	Ent-kaurene synthase 1 (KS)	9.53	8.75	8.23	11.12	11.21	13.53	Up
Cla020710	Ent-kaurene oxidase (KO)	12.92	13.62	10.71	28.40	24.53	29.08	Up (sig)
Cla006992	Ent-kaurenoic acid oxidase 1 (KAO)	14.56	24.91	31.02	23.16	16.90	20.05	Down
Cla021351	Ent-kaurenoic acid oxidase 1 (KAO)	1.66	1.41	1.27	1.72	1.20	1.42	-
Cla002362	Gibberellin 20-oxidase (GA20ox)	1.39	0.43	1.08	9.77	10.05	10.28	Up (sig)
Cla006227	Gibberellin 20-oxidase (GA20ox)	0.00	0.00	0.00	0.71	0.16	0.38	Up (sig)
Cla006941	Gibberellin 20-oxidase (GA20ox)	0.47	0.52	1.17	1.03	0.30	0.44	Down
Cla008413	Gibberellin 20-oxidase (GA20ox)	0.00	0.00	0.04	0.28	0.18	0.67	Up (sig)
Cla010726	Gibberellin 20-oxidase-like protein (GA20ox)	3.98	3.64	3.63	5.68	5.27	5.58	Up
Cla013892	Gibberellin 20-oxidase (GA20ox)	0.09	0.16	0.04	0.19	0.18	0.26	Up
Cla015407	Gibberellin 3-beta-hydroxylase (GA3ox)	4.56	3.86	4.13	11.86	12.36	10.67	Up (sig)
Cla022285	Gibberellin 3-beta-hydroxylase (GA3ox)	0.05	0.00	0.00	0.30	0.14	0.04	Up
Cla005259	Gibberellin 2-beta-dioxygenase 8 (GA2ox)	0.00	0.00	0.19	0.00	0.11	0.52	Up
Cla005397	Gibberellin 2-oxidase (GA2ox)	2.92	8.67	2.63	3.29	4.50	2.05	Down
Cla007482	Gibberellin 2-beta-dioxygenase 8 (GA2ox)	1.53	1.35	1.24	1.13	1.31	1.95	Up
Cla009774	Gibberellin 2-oxidase (GA2ox)	0.00	0.18	0.17	0.27	0.36	0.05	Up
Cla015162	Gibberellin 2-oxidase (GA2ox)	0.05	0.05	0.00	0.84	0.72	0.75	Up (sig)
Cla017338	Gibberellin 2-oxidase 2 (GA2ox)	0.00	0.00	0.05	0.62	0.03	0.20	Up
Cla019586	Gibberellin 2-oxidase (GA2ox)	0.32	1.53	0.87	6.71	3.51	9.32	Up (sig)

Table 4. Expression of GA biosynthetic and metabolic genes by transcriptome analysis. ‘V’ indicates the vine plants in the F₂ population; ‘D’ indicates the dwarf plants in the F₂ population; ‘up/down’ indicates the up/down-regulation of genes in dwarf plants compared with the vine plants; ‘sig’ indicates the significantly up/down-regulated gene. The table listed the genes expressed at least a library and those GA biosynthetic and metabolic genes did not express in any library were not listed.

proteins (Cla002362, Cla006227, Cla006941, Cla008413 and Cla013892) and two Arabidopsis GA20ox proteins (AT5G07200 and AT1G44090). Subgroup II contained five watermelon GA2ox proteins (Cla015162, Cla017338, Cla005397, Cla009774 and Cla019586) and two Arabidopsis GA2ox proteins (AT1G47990 and AT1G30040). Subgroup III contained two GA3ox proteins (Cla022285 and Cla015407), two GA2ox proteins (Cla005259 and Cla007482) from watermelon and two GA3ox proteins (AT4G21690 and AT1G15550) from Arabidopsis. However, Cla010726, encoding the gibberellin 20-oxidase-like protein, did not belong to any of these subgroups.

Endogenous levels of GAs were changed in the dwarf plants. Except for GA₇, the remaining 17 kinds of GAs were detected from the shoots of vine and dwarf plants in two parents and F₂ population using the 2H₂-GA internal standards coupled with UPLC-MS/MS analyses. Among these GAs, endogenous level of GA₃ was significantly increased and GA₄ was significantly decreased in dwarf plants of two parents and F₂ population (Table 5). Additionally, endogenous levels of GA₉ and GA₂₉ were significantly increased in dwarf plants of F₂ population. The results indicated the reduced level of bioactive GA₄ might be the main cause for the dwarf phenotype in watermelon (Table 5).

Moreover, we constructed the GA biosynthetic and metabolic pathway combining the endogenous levels of GAs and genes involved in this pathway (Fig. 5). Two major pathways, GA₅₃-pathway (involving GA₅₃, GA₄₄, GA₁₉, GA₂₀, GA₁, GA₈, GA₂₉, GA₅, GA₃ and GA₆) and GA₁₂-pathway (involving GA₁₂, GA₁₅, GA₂₄, GA₉, GA₄, GA₃₄, GA₅₁ and GA₇), were included. The GA₉ and GA₄ in the GA₁₂-pathway showed different changes of endogenous levels between the vine and dwarf plants (Fig. 5; Table 5). Endogenous level of GA₉ was increased in dwarf plants of F₂ population, which might be due to the increased expression level of GA20ox genes (Cla002362, Cla006227 and Cla008413) in dwarf plants as indicated in Table 4. Endogenous level of bioactive GA₄ was decreased in dwarf plants, suggesting the mutation of Cla015407 (GA3ox) impaired the biosynthesis of GA₄ in GA₁₂-pathway. Endogenous level of GA₂₉ and GA₃ in the GA₅₃-pathway were increased in dwarf plants (Fig. 5; Table 5). The increased GA₂₉ content might be attributed to the increased expression level of GA2ox genes (Cla015162 and Cla019586) in dwarf plants as indicated in Table 4. Endogenous level of bioactive GA₃ was increased in dwarf plants, which might be due to the up-regulation of another GA3ox paralogue, Cla022285, as a result of feedback of reduced GA₄ content caused by the mutation of Cla015407 (GA3ox) (Table 4).

Exogenous GA applications can rescue the dwarf phenotype. We investigated the responses of dwarf plants to 500 μM GA₃ and 500 μM GA₄₊₇ applications and found that the independent applications of GA₃ or GA₄₊₇ could both rescue the dwarf phenotype in watermelon (Fig. 6). Moreover, GA₄₊₇ treatments had a more distinct effect than GA₃ treatments, resulting in greater plant height (Fig. 6). These observations further verified that the *Si* gene is a GA biosynthetic gene.

Types of GAs	CG, vine parent (\pm SD)	w106, dwarf parent (\pm SD)	Vine plants of F ₂ population (\pm SD)	Dwarf plants of F ₂ population (\pm SD)
GA ₁	0.0152 \pm 0.0003	0.0210 \pm 0.0016	0.0270 \pm 0.0007	0.0230 \pm 0.0004
GA ₃	n.d	0.0527 \pm 0.0027* \uparrow	0.0268 \pm 0.0010	0.1029 \pm 0.0034* \uparrow
GA ₄	0.1074 \pm 0.0026	0.0118 \pm 0.0011* \downarrow	0.0900 \pm 0.0064	0.0176 \pm 0.0016* \downarrow
GA ₅	0.0223 \pm 0.0020	0.0225 \pm 0.0006	0.0216 \pm 0.0007	0.0217 \pm 0.0009
GA ₆	0.0081 \pm 0.0002	0.0100 \pm 0.0012	n.d	0.0084 \pm 0.0014
GA ₇	n.q	n.q	n.d	n.q
GA ₈	0.0256 \pm 0.0039	0.0275 \pm 0.0018	0.0275 \pm 0.0009	0.0325 \pm 0.0028
GA ₉	0.0494 \pm 0.0016	0.0452 \pm 0.0016	0.0371 \pm 0.0012	0.0992 \pm 0.0046* \uparrow
GA ₁₂	0.0882 \pm 0.0088	0.0516 \pm 0.0044	0.0466 \pm 0.0080	0.0362 \pm 0.0014
GA ₁₅	n.d	0.0882 \pm 0.0025	n.d	n.d
GA ₁₉	0.1935 \pm 0.0135	0.3053 \pm 0.0220	0.1906 \pm 0.0208	0.1770 \pm 0.0183
GA ₂₀	0.0394 \pm 0.0081	0.0309 \pm 0.0011	0.0329 \pm 0.0034	0.0469 \pm 0.0038
GA ₂₄	0.0800 \pm 0.0013	0.0652 \pm 0.0019	0.0633 \pm 0.0021	0.0575 \pm 0.0022
GA ₂₉	0.0607 \pm 0.0015	0.1136 \pm 0.0018	0.0549 \pm 0.0005	0.2391 \pm 0.0045* \uparrow
GA ₃₄	0.0364 \pm 0.0023	n.d	n.d	n.q
GA ₄₄	0.1218 \pm 0.0017	0.1695 \pm 0.0158	0.1193 \pm 0.0075	n.q
GA ₅₁	0.0187 \pm 0.0016	0.0277 \pm 0.0025	0.0239 \pm 0.0024	0.0263 \pm 0.0034
GA ₅₃	0.0093 \pm 0.0005	0.0152 \pm 0.0011	0.0058 \pm 0.0008	0.0044 \pm 0.0008

Table 5. Measurement of endogenous levels (ng/g fresh weight) of GAs in dwarf and vine plants in two parents and F₂ population using 2H₂-GA internal standards coupled with UPLC-MS/MS analyses. Mean values of three independent UPLC-MS/MS runs. *Means GA level between two parents and the dwarf and vine plants in F₂ population are significantly different at $p < 0.05$ by T-test using SAS 8.0 and $|\log_2\text{Fold(FC)}| \geq 1$. SD means standard deviation. 'n.d.' means no decision and 'n.q.' means no quantitation.

Subcellular localization of GA3ox proteins. The subcellular localization of GA3ox proteins from 'CG' and 'w106', namely CG-Cla015407, w106-Cla015407-Iso1, and w106-Cla015407-Iso2, were analyzed by transient expression of the green fluorescent protein (GFP) fusion proteins in tobacco leaf epidermal cells. As shown in Fig. 7, all of the three GA3ox proteins were localized in the nucleus and cytosol.

Discussion

Plant height, as the key component of plant architecture, has been associated with both natural beauty and yield performance. Total cell number and cell size, resulting from cell division and expansion, determine the size of plant organs⁵⁶. For example, the average cell size of the cucumber dwarf mutant *scp2* was significantly smaller than that of wild type plants⁵⁷. The cucumber *Csdw* mutant showed dwarfing phenotype and decreased internode length due to the reduced cell division in main stem⁵⁸. The rice *stemless dwarf 1 (std1)* mutant showed severe dwarfing phenotype, abnormal cell morphology and reduced cell division rate⁵⁹. Further analyses revealed that a large number of cells were blocked in the S and G₂/M phases, with the presence of many multinucleate cells⁵⁹. In present study, microscopic observations of stem transverse and longitudinal sections revealed that the reduced plant height could be mainly attributed to the shorter longitudinal cell lengths (Fig. 1b,c).

Genetic mapping and identification of dwarfism genes have occurred in cucurbits, such as *scp-2*⁵⁷, *Csdw*⁵⁸, *cp*⁶⁰ and *scp-1*⁶¹ in cucumber; *mdw1*⁶² in melon; and *qCmB263* in pumpkin. In watermelon, the genes of *dsh*³⁷, *Cldf*³⁸, *dw*³⁹ and *Cldw-1*⁴⁰, conferring dwarf phenotypes, were studied and identified. NGS-assisted BSA is an effective method to identify target genes controlling the dwarf traits by genotyping the bulked DNA samples having distinct or opposite extreme phenotypes in plants³⁸. In this study, we employed the BSA-Seq to identify the candidate gene controlling the dwarf trait in watermelon and delimited the region to 0.80–3.43 Mb on chromosome 9 (Fig. 2a–c). A further mapping analysis finally located this gene in a 541-kb interval (Fig. 2d), with Cla015407 (*GA3ox*) being the candidate gene.

GA3ox catalyzes the last step of bioactive GA synthesis, which converts GA₂₀ to GA₁, GA₅ to GA₃, and GA₉ to GA₄¹⁸. Mutations in *GA3ox* genes, such as *dwarf1 (d1)* from maize¹⁸, *dwarf18 (d18)* from rice²⁶, *GA4* from Arabidopsis²⁷, *Msdw1* from *Medicago sativa*²⁸, and *le* from pea⁶⁴, resulted in dwarfism. For example, the coding sequences of *GA3ox2* isolated from *d18* alleles were analyzed in rice. In the strong allele, *d18-Id18^h*, the deletion of a guanine base at 750 altered the reading frame, and in the weak allele, *d18-dy*, the 9-bp deletion deleted three amino acids²⁶. The dwarf mutant *Msdw1* had an amino acid change in a conserved position of the *GA3ox* gene compared with the wild type in *Medicago sativa*²⁸. Sequence alignment revealed a G-to-A transition conferring an alanine-to-threonine substitution at residue 229 in the *le* gene product in pea⁶⁴. The same locus of *GA3ox*, Cla015407, conferring the dwarf phenotypes in watermelon were concurrently identified in this study and those of Wei et al³⁸ and Gebremeskel et al³⁹. Additionally, the SNP mutation (G \rightarrow A) at position 626 of DNA sequence, locating at the splice acceptor site of intron, was simultaneously detected in our study and those of Wei et al³⁸ and Gebremeskel et al³⁹. Similar with previous reports, the SNP mutation leading to 13-bp deletion in the second exon of *GA3ox* transcript, was also observed in our dwarf parent 'w106'. Moreover, another *GA3ox* transcript

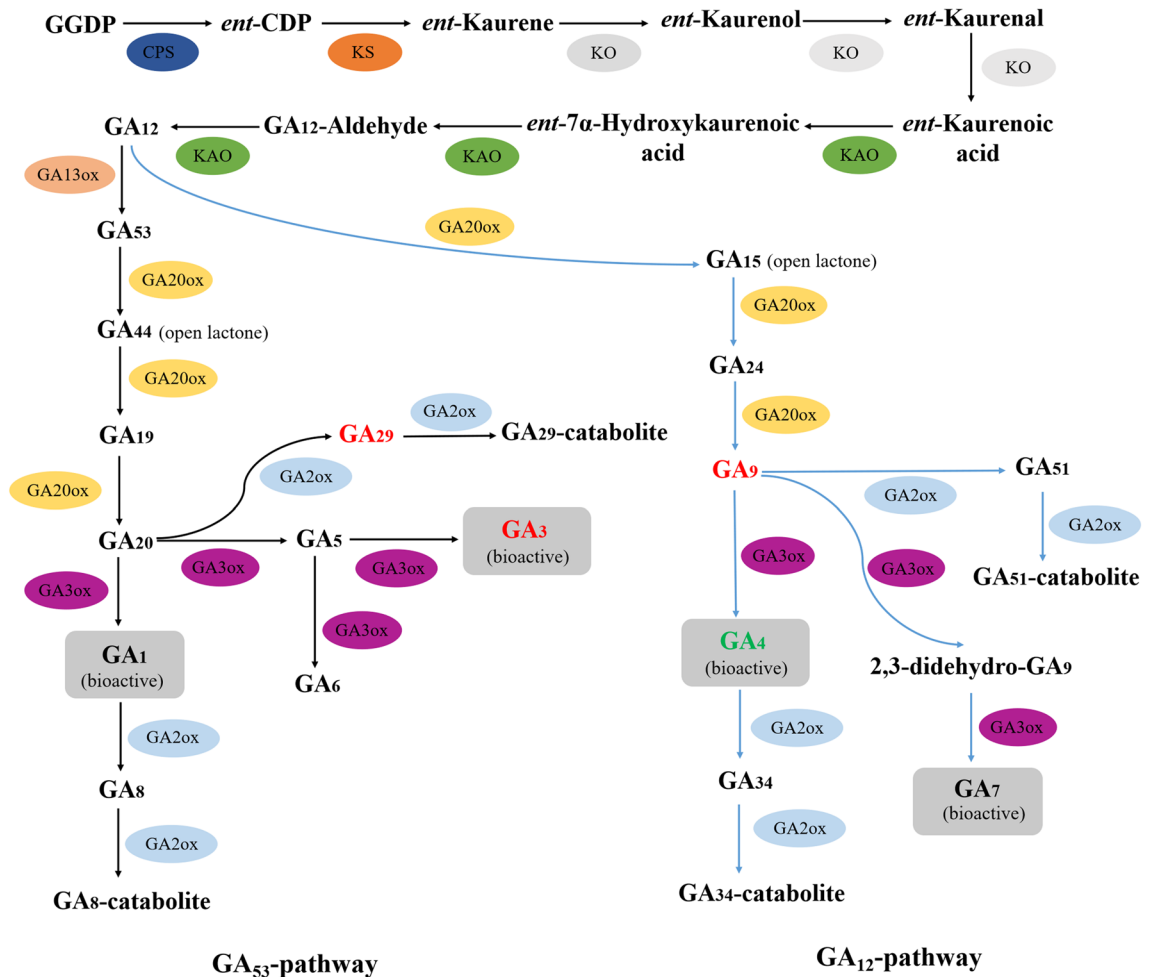


Figure 5. The predicted pathways of GA biosynthesis and metabolism in watermelon. The pathways were constructed according to the previous reports of GA biosynthetic and metabolic pathways in higher plants. Two major pathways, GA₅₃-pathway and GA₁₂-pathway were present in watermelon. The levels of GA₃ and GA₂₉ in GA₅₃-pathway were increased in dwarf plants and marked with red color. The level of GA₉ in GA₁₂-pathway was increased and marked with red color, and level of GA₄ in GA₁₂-pathway was decreased in dwarf plants and marked with green color.

caused by this point mutation, which retained the intron sequence, was identified in our dwarf parent ‘w106’. However, this full-length isoform was not present in the dwarf parents ‘N21’ and ‘Duan125’ of Wei et al³⁸ and Gebremeskel et al³⁹.

In the present study, the candidate gene, Cla015407 (*GA3ox*), significantly increased the expression level in dwarf plants compared with the vine plants (Table 4). Additionally, one *KO* gene (Cla020710), three *GA20ox* genes (Cla002362, Cla006227 and Cla008413) and two *GA2ox* genes (Cla015162 and Cla019586) were also significantly up-regulated in dwarf plants (Table 4). The increased expression of GA related genes in this study were partially consistent with Wei et al³⁸, in which the *GA3ox* (Cla015407), *CPS* (Cla006048), *KAO* (Cla021351, Cla006992 and Cla016164), and *GA20ox* (Cla002362, Cla006227 and Cla010726) were significantly up-regulated in dwarf line ‘N21’. Different from our results, the expression of *GA3ox* (Cla015407) in the dwarf parent ‘Duan125’ was significantly reduced according to the report of Gebremeskel et al.³⁹. The increase in expression of GA related genes in our study might be due to the feedback of low levels of bioactive GA₄ in dwarf plants as showing in Table 5. This is a well-known phenomenon whereby mutations or chemical intervention in GA biosynthesis or GA perception result in increases in *GA20ox* and *GA3ox* in a homeostatic mechanism¹⁴. Moreover, two transcripts of *GA3ox*, the intron retention isoform and 13-bp deletion isoform, were generated in the dwarf parent ‘w106’ in our study. Introns are often added to increase expression, although the mechanism through introns stimulate gene expression in plants remains unclear⁶⁵. For instance, inserting the first intron from the *UBQ10* gene into intronless genes markedly increased the latter’s mRNA accumulation to over 150-fold in *Arabidopsis*⁶⁵. Therefore, the up-regulated *GA3ox* gene might also be attributed to altered splicing event in dwarf plants.

Endogenous levels of GAs were measured using 2H₂-GA internal standards and UPLC-MS/MS and we find that GA₃, GA₉ and GA₂₉ were significantly increased and GA₄ was significantly decreased in dwarf plants (Fig. 5; Table 5). The results were different from a previous study of Gebremeskel et al³⁹, in which significantly lower GA₃ content was obtained in the dwarf parent ‘Duan125’ of watermelon. The increased content of GA₉ in GA₁₂-pathway might be resulted from the up-regulation of *GA20ox* genes (Cla002362, Cla006227 and Cla010726)

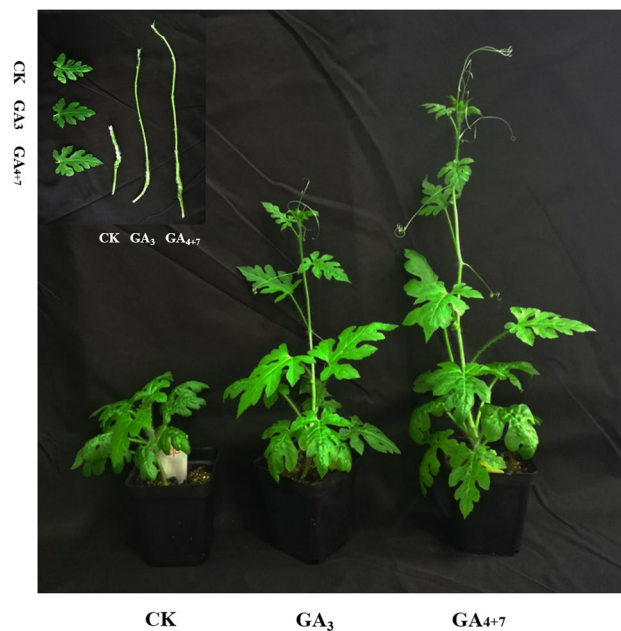


Figure 6. Dwarf architecture could be rescued after GA_3 or GA_{4+7} treatment.

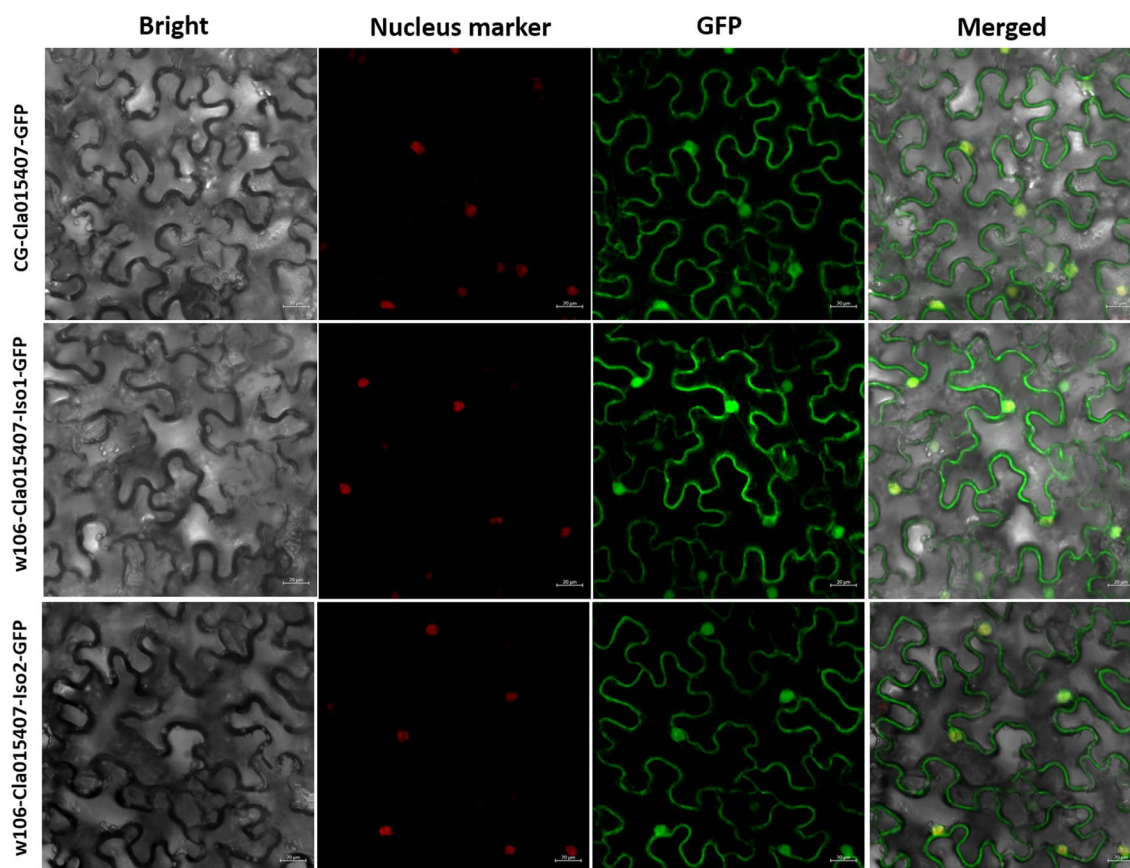


Figure 7. Subcellular localization of $GA3ox$ proteins from two parental lines. Green fluorescent protein (GFP)-fusion proteins were transiently expressed in tobacco leaf epidermal cells. After 48 h of incubation, GFP signal was detected with a fluorescence microscope. Bright-field, nucleus marker, fluorescence, and merged images of CG-Cla015407-GFP, w106-Cla015407-Iso1-GFP, and w106-Cla015407-Iso2-GFP were shown.

in dwarf plants, and the reduced content of bioactive GA₄ indicated that loss function of *GA3ox* (Cla015407) impaired the GA₄ biosynthesis in GA₁₂-pathway. Furthermore, GA₅₁ content in GA₁₂-pathway was increased in dwarf plants, however, not to a significant level. The results indicate that mutation of *GA3ox* (Cla015407) promotes the biosynthesis of GA₅₁ and inhibits the biosynthesis of GA₄ from GA₉ in GA₁₂-pathway. Moreover, endogenous level of GA₂₉ in GA₅₃-pathway was increased, which might be attributed to the increased expression level of *GA2ox* genes (Cla015162 and Cla019586) in dwarf plants. Additionally, endogenous level of bioactive GA₃ in GA₅₃-pathway was increased in dwarf plants, which aroused our interest. We speculated that the reduction in GA₄ level in GA₁₂-pathway resulted in increased expression, through release of feedback, of another *GA3ox* paralogue, Cla022285, with the ability to produce GA₃ in GA₅₃-pathway (Table 4; Fig. 5). In rice, two *GA3ox* genes, *OsGA3ox1* and *OsGA3ox2*, have the activity for converting GA₂₀ to GA₁, GA₅ to GA₃, GA₄₄ to GA₃₈, and GA₉ to GA₄²⁶. Additionally, the maize *dwarf-1* gene (putative GA 3β-hydroxylase) controls the three biosynthetic steps: GA₂₀ to GA₁, GA₂₀ to GA₅, and GA₅ to GA₃⁶⁶. However, there is no evidence that Cucurbits contains such an *GA3ox* enzyme currently⁶⁷. In cucumber, four GA 3-oxidases (CsGA3ox1, -2, -3, and -4) were identified and all these GA 3-oxidases oxidized the C₁₉-GA GA₉ to GA₄ as the only product⁶⁷. In this study, the presences of GA₁, GA₅, GA₆, GA₃ and GA₄ indicate that the *GA3ox* proteins have the activity for catalyzing GA₂₀ to GA₁, GA₂₀ to GA₅, GA₅ to GA₆, GA₅ to GA₃, and GA₉ to GA₄, and the absence of GA₇ suggests that the *GA3ox* proteins do not have 2,3-desaturation activity in watermelon.

The rescue of the dwarf phenotype has been reported in GA-deficient mutants in plants. For instance, the application of GA₃ could partially rescue the dwarf phenotype of the cucumber mutant *Csdw*⁵⁸. In watermelon, the dwarf phenotypes of *Cldf* and *dw* could be rescued by exogenous GA₃ application^{38,39}. In the present study, exogenous applications of GA₃ or GA₄₊₇ could rescue the height of dwarf plants, with the latter have a more distinct affect than the former (Fig. 6). The results further confirmed the *Si* gene is a GA biosynthetic gene and the dwarf phenotype might be attributed to the reduced GA₄ level.

Accession of sequencing data

Whole-genome sequencing data from this study can be accessed at sequence read archive (SRA) database from NCBI (<https://www.ncbi.nlm.nih.gov/sra>) with accession number SRR8893166 (female parent 'w106'), SRR8893167 (male parent 'Charleston Gray'), SRR8893168 (dwarf bulk) and SRR8893169 (vine bulk).

Received: 27 December 2019; Accepted: 18 August 2020

Published online: 10 September 2020

References

1. Würschum, T., Langer, S. M., Longin, C. F. H., Tucker, M. R. & Leiser, W. L. A modern Green Revolution gene for reduced height in wheat. *Plant J.* **92**, 892–903 (2017).
2. Wing, R. A., Purugganan, M. D. & Zhang, Q. The rice genome revolution: From an ancient grain to Green Super Rice. *Nat. Rev. Genet.* **19**, 505–517 (2018).
3. Peng, J. *et al.* “Green revolution” genes encode mutant gibberellin response modulators. *Nature* **400**, 256–261 (1999).
4. Nomura, T. *et al.* Brassinosteroid deficiency due to truncated steroid 5α-reductase causes dwarfism in the *lk* mutant of pea. *Plant Physiol.* **135**, 2220–2229 (2004).
5. Cheng, J. *et al.* A single nucleotide mutation in *GID1c* disrupts its interaction with *DELLA1* and causes a GA-insensitive dwarf phenotype in peach. *Plant Biotech. J.* **17**, 1723–1735 (2019).
6. Ford, B. A. *et al.* *Rht18* semidwarfism in wheat is due to increased *GA 2-oxidaseA9* expression and reduced GA content. *Plant Physiol.* **177**, 168–180 (2018).
7. Castorina, G. *et al.* The maize lilliputian1 (*lil1*) gene, encoding a brassinosteroid cytochrome P450 C-6 oxidase, is involved in plant growth and drought response. *Ann. Bot.* **122**, 227–238 (2018).
8. Li, H. *et al.* An auxin signaling gene *BnaA3.LAA7* contributes to improved plant architecture and yield heterosis in rapeseed. *New Phytol.* **222**, 837–851 (2019).
9. Jiang, L. *et al.* *DWARF 53* acts as a repressor of strigolactone signalling in rice. *Nature* **504**, 401–405 (2013).
10. Chen, W. *et al.* Small Grain and Dwarf 2, encoding an HD-Zip II family transcription factor, regulates plant development by modulating gibberellin biosynthesis in rice. *Plant Sci.* **288**, 110208. <https://doi.org/10.1016/j.plantsci.2019.110208> (2019).
11. Wang, W. *et al.* Dwarf tiller1, a wuschel-related homeobox transcription factor, is required for tiller growth in rice. *PLoS Genet.* **10**, e1004154. <https://doi.org/10.1371/journal.pgen.1004154> (2014).
12. Magome, H., Yamaguchi, S., Hanada, A., Kamiya, Y. & Oda, K. Dwarf and delayed-flowering 1, a novel Arabidopsis mutant deficient in gibberellin biosynthesis because of overexpression of a putative *AP2* transcription factor. *Plant J.* **37**, 720–729 (2004).
13. Zhou, S. *et al.* Manipulation of plant architecture and flowering time by down-regulation of the GRAS transcription factor *SIGRAS26* in *Solanum lycopersicum*. *Plant Sci.* **271**, 81–93 (2018).
14. Hedden, P. & Phillips, A. L. Gibberellin metabolism: New insights revealed by the genes. *Trends Plant Sci.* **5**, 523–530 (2000).
15. Yamaguchi, S. Gibberellin metabolism and its regulation. *Annu. Rev. Plant Biol.* **59**, 225–251 (2008).
16. Sun, T. P. Gibberellin-GID1-DELLA: A pivotal regulatory module for plant growth and development. *Plant Physiol.* **154**, 567–570 (2010).
17. Qin, X. *et al.* Gibberellin 20-oxidase gene *OsGA20ox3* regulates plant stature and disease development in rice. *Mol. Plant Microbe Interact.* **26**, 227–239 (2013).
18. Chen, Y. *et al.* The maize *DWARF1* encodes a gibberellin 3-oxidase and is dual localized to the nucleus and cytosol. *Plant Physiol.* **166**, 2028–2039 (2014).
19. Thomas, S. G., Phillips, A. L. & Hedden, P. Molecular cloning and functional expression of gibberellin 2-oxidases, multifunctional enzymes involved in gibberellin deactivation. *Proc. Natl. Acad. Sci. USA* **96**, 4698–4703 (1999).
20. Oikawa, T., Koshioka, M., Kojima, K., Yoshida, H. & Kawata, M. A role of *OsGA20ox1*, encoding an isoform of gibberellin 20-oxidase, for regulation of plant stature in rice. *Plant Mol. Biol.* **55**, 687–700 (2004).
21. Spielmeier, W., Ellis, M. H. & Chandler, P. M. Semidwarf (*sd-1*), “green revolution” rice, contains a defective gibberellin 20-oxidase gene. *Proc. Natl. Acad. Sci. USA* **99**, 9043–9048 (2002).
22. Xu, Y. *et al.* Characterization of the *sdw1* semi-dwarf gene in barley. *BMC Plant Biol.* **17**, 11. <https://doi.org/10.1186/s12870-016-0964-4> (2017).

23. Teplyakova, S. *et al.* Impact of the 7-bp deletion in HvGA20ox2 gene on agronomic important traits in barley (*Hordeum vulgare* L.). *BMC Plant Biol.* **17**, 181. <https://doi.org/10.1186/s12870-017-1121-4> (2017).
24. Xu, Y. L. *et al.* The GA5 locus of *Arabidopsis thaliana* encodes a multifunctional gibberellin 20-oxidase: Molecular cloning and functional expression. *Proc. Natl. Acad. Sci. USA* **92**, 6640–6644 (1995).
25. Luo, Y. *et al.* A single nucleotide deletion in gibberellin 20-oxidase1 causes alpine dwarfism in *Arabidopsis*. *Plant Physiol.* **168**, 930–937 (2015).
26. Itoh, H., Ueguchi-Tanaka, M., Sentoku, N., Kitano, H. & Matsuoka, M. M. K. Cloning and functional analysis of two gibberellin 3 β -hydroxylase genes that are differently expressed during the growth of rice. *Proc. Natl. Acad. Sci. USA* **98**, 8909–8914 (2001).
27. Chiang, H. H., Hwang, I. & Goodman, H. M. Isolation of the *Arabidopsis* GA4 locus. *Plant Cell* **7**, 195–201 (1995).
28. Dalmadi, A. *et al.* Dwarf plants of diploid *Medicago sativa* carry a mutation in the gibberellin 3- β -hydroxylase gene. *Plant Cell Rep.* **27**, 1271–1279 (2008).
29. Wuddineh, W. A. *et al.* Identification and overexpression of gibberellin 2-oxidase (GA2ox) in switchgrass (*Panicum virgatum* L.) for improved plant architecture and reduced biomass recalcitrance. *Plant Biotechnol. J.* **13**, 636–647 (2015).
30. Liu, C. *et al.* Shortened basal internodes encodes a gibberellin 2-oxidase and contributes to lodging resistance in rice. *Mol. Plant* **11**, 288–299 (2018).
31. Schragar-Lavelle, A. *et al.* The role of a class III gibberellin 2-oxidase in tomato internode elongation. *Plant J.* **97**, 603–615 (2019).
32. Guo, S. *et al.* The draft genome of watermelon (*Citrullus lanatus*) and resequencing of 20 diverse accessions. *Nat. Genet.* **45**, 51–58 (2013).
33. Mohr, H. C. Mode of inheritance of the bushy growth characteristics in watermelon. *Proc. Assoc. South Agric. Work* **53**, 174 (1956).
34. Dyutin, K. E. & Afanaseva, E. A. Inheritance of the short vine trait in watermelon. *Cytol. Genet.* **21**, 71–73 (1987).
35. Liu, P. B. W. & Loy, J. B. Action of gibberellic acid on cell proliferation in the subapical shoot meristem of watermelon seedlings. *Am. J. Bot.* **63**, 700–704 (1976).
36. Huang, H. X., Zhang, X. Q., Wei, Z. C., Li, Q. H. & Li, X. Inheritance of male-sterility and dwarfism in watermelon [*Citrullus lanatus* (Thunb.) Matsum and Nakai]. *Sci. Hortic.* **74**, 175–181 (1998).
37. Dong, W., Wu, D., Li, G., Wu, D. & Wang, Z. Next-generation sequencing from bulked segregant analysis identifies a dwarfism gene in watermelon. *Sci. Rep.* **8**, 2908. <https://doi.org/10.1186/s12870-016-0964-4> (2018).
38. Wei, C. *et al.* A point mutation resulting in a 13 bp deletion in the coding sequence of Clf leads to a GA-deficient dwarf phenotype in watermelon. *Hortic. Res.* **6**, 132. <https://doi.org/10.1038/s41438-019-0213-8> (2019).
39. Gebremeskel, H. *et al.* Molecular mapping and candidate gene analysis for GA₃ responsive short internode in watermelon (*Citrullus lanatus*). *Int. J. Mol. Sci.* **21**, 290. <https://doi.org/10.3390/ijms21010290> (2019).
40. Zhu, H. *et al.* A single nucleotide deletion in an ABC transporter gene leads to a dwarf phenotype in watermelon. *Front Plant Sci.* **10**, 1399. <https://doi.org/10.3389/fpls.2019.01399> (2019).
41. Wei, C. *et al.* Genetic mapping of the LOBED LEAF 1 (CILL1) gene to a 127.6-kb region in watermelon (*Citrullus lanatus* L.). *PLoS ONE* **12**, e0180741. <https://doi.org/10.1371/journal.pone.0180741> (2017).
42. Dou, J. *et al.* Genetic mapping reveals a marker for yellow skin in watermelon (*Citrullus lanatus* L.). *PLoS One* **13**, e0200617. <https://doi.org/10.1371/journal.pone.0200617> (2018).
43. Dou, J. *et al.* Genetic mapping reveals a candidate gene (ClFS1) for fruit shape in watermelon (*Citrullus lanatus* L.). *Theor. Appl. Genet.* **131**, 947–958 (2018).
44. Oren, E. *et al.* The multi-allelic APRR2 gene is associated with fruit pigment accumulation in melon and watermelon. *J. Exp. Bot.* **70**, 3781–3794 (2019).
45. Jang, Y. J. *et al.* An evolutionarily conserved non-synonymous SNP in a leucine-rich repeat domain determines anthracnose resistance in watermelon. *Theor. Appl. Genet.* **132**, 473–488 (2019).
46. Li, H. & Durbin, R. Fast and accurate short read alignment with Burrows–Wheeler transform. *Bioinformatics* **25**, 1754–1760 (2009).
47. Li, H. *et al.* The sequence alignment/map format and SAM tools. *Bioinformatics* **25**, 2078–2079 (2009).
48. de Valle, I. F. *et al.* Optimized pipeline of MuTect and GATK tools to improve the detection of somatic single nucleotide polymorphisms in whole-exome sequencing data. *BMC Bioinf.* **17**, 341. <https://doi.org/10.1186/s12859-016-1190-7> (2016).
49. Wang, K., Li, M. & Hakonarson, H. ANNOVAR: Functional annotation of genetic variants from high-throughput sequencing data. *Nucleic Acids Res.* **38**, e164. <https://doi.org/10.1093/nar/gkq603> (2010).
50. Abe, A. *et al.* Genome sequencing reveals agronomically important loci in rice using MutMap. *Nat. Biotechnol.* **30**, 174–178 (2012).
51. She, H. *et al.* Fine mapping and candidate gene screening of the downy mildew resistance gene RPF1 in Spinach. *Theor. Appl. Genet.* **131**, 2529–2541 (2018).
52. Geng, X. *et al.* Rapid identification of candidate genes for seed weight using the SLAF-Seq method in *Brassica napus*. *PLoS One* **11**, e0147580. <https://doi.org/10.1371/journal.pone.0147580> (2016).
53. Singh, V. K. *et al.* Indel-seq: A fast-forward genetics approach for identification of trait-associated putative candidate genomic regions and its application in pigeonpea (*Cajanus cajan*). *Plant Biotechnol. J.* **15**, 906–914 (2017).
54. Trapnell, C. *et al.* Transcript assembly and quantification by RNA Seq reveals unannotated transcripts and isoform switching during cell differentiation. *Nat. Biotechnol.* **28**, 511–515 (2010).
55. Kanehisa, M. & Goto, S. KEGG: Kyoto encyclopedia of genes and genomes. *Nucleic Acids Res.* **28**, 27–30 (2000).
56. Breuninger, H. & Lenhard, M. Control of tissue and organ growth in plants. *Curr. Top. Dev. Biol.* **91**, 185–220 (2010).
57. Hou, S. *et al.* A mutant in the CsDET2 gene leads to a systemic brassinosteroid deficiency and super compact phenotype in cucumber (*Cucumis sativus* L.). *Theor. Appl. Genet.* **130**, 1693–1703 (2017).
58. Xu, L., Wang, C., Cao, W., Zhou, S. & Wu, T. CLAVATA1-type receptor-like kinase CsCLAVATA1 is a putative candidate gene for dwarf mutation in cucumber. *Mol. Genet. Genom.* **293**, 1393–1405 (2018).
59. Fang, J. *et al.* Reduction of ATPase activity in the rice kinesin protein Stemless Dwarf 1 inhibits cell division and organ development. *Plant J.* **96**(3), 620–634 (2018).
60. Li, Y. *et al.* Fine genetic mapping of cp: A recessive gene for compact (dwarf) plant architecture in cucumber, *Cucumis sativus* L.. *Theor. Appl. Genet.* **123**, 973–983 (2011).
61. Wang, H. *et al.* The cytochrome P450 gene CsCYP85A1 is a putative candidate for super compact-1 (Scp-1) plant architecture mutation in cucumber (*Cucumis sativus* L.). *Front. Plant Sci.* **8**, 266. <https://doi.org/10.3389/fpls.2017.00266> (2017).
62. Hwang, J. *et al.* Fine genetic mapping of a locus controlling short internode length in melon (*Cucumis melo* L.). *Mol. Breed.* **34**, 949–961 (2014).
63. Zhang, G. *et al.* A high-density genetic map for anchoring genome sequences and identifying QTLs associated with dwarf vine in pumpkin (*Cucurbita maxima* Duch.). *BMC Genom.* **16**, 1101. <https://doi.org/10.1186/s12864-015-2312-8> (2015).
64. Lester, D. R., Ross, J. J., Davies, P. J. & Reid, J. B. Mendel's stem length gene (*Le*) encodes a gibberellin 3 β -hydroxylase. *Plant Cell* **9**, 1435–1443 (1997).
65. Emami, S., Arumainayagam, D., Korf, I. & Rose, A. B. The effects of a stimulating intron on the expression of heterologous genes in *Arabidopsis thaliana*. *Plant Biotechnol. J.* **11**, 555–563 (2013).
66. Spray, C. R. *et al.* The dwarf-1 (dt) mutant of *Zea mays* blocks three steps in the gibberellin-biosynthetic pathway. *Proc. Natl. Acad. Sci. USA* **93**, 10515–10518 (1996).
67. Pimenta Lange, M. J. *et al.* Functional characterization of gibberellin oxidases from cucumber, *Cucumis sativus* L.. *Phytochemistry* **90**, 62–69 (2013).

Acknowledgements

This work was funded by the Youth Talents Training Program of Zhejiang Academy of Agricultural Sciences (2019R23R08E01). We thank Lesley Benyon, PhD, from Liwen Bianji, Edanz Group China (www.liwenbianji.cn/ac), for editing the English text of a draft of this manuscript.

Author contributions

Y.Y.S. and M.F. conceived and designed the experiment. M.F. constructed the F₁ and F₂ progeny. Y.Y.S. carried out the bioinformatics analysis. Y.Y.S. and H.Q.Z. carried out the experimental analysis. Y.Y.S. wrote the manuscript, and M.F., Y.J.H., and P.A.G. gave insightful suggestions.

Competing interests

The authors declare no competing interests.

Additional information

Supplementary information is available for this paper at <https://doi.org/10.1038/s41598-020-71861-7>.

Correspondence and requests for materials should be addressed to M.F.

Reprints and permissions information is available at www.nature.com/reprints.

Publisher's note Springer Nature remains neutral with regard to jurisdictional claims in published maps and institutional affiliations.



Open Access This article is licensed under a Creative Commons Attribution 4.0 International License, which permits use, sharing, adaptation, distribution and reproduction in any medium or format, as long as you give appropriate credit to the original author(s) and the source, provide a link to the Creative Commons licence, and indicate if changes were made. The images or other third party material in this article are included in the article's Creative Commons licence, unless indicated otherwise in a credit line to the material. If material is not included in the article's Creative Commons licence and your intended use is not permitted by statutory regulation or exceeds the permitted use, you will need to obtain permission directly from the copyright holder. To view a copy of this licence, visit <http://creativecommons.org/licenses/by/4.0/>.

© The Author(s) 2020